J Fluoresc (2015) 25:95–102
DOI 10.1007/s10895-014-1484-y

ORIGINAL PAPER

Multiple Linear Regression Solvatochromic Analysis of Donar-Acceptor Imidazole Derivatives

J. Jayabharathi · V. Thanikachalam · V. Kalaiarasi · P. Ramanathan

Received: 31 July 2014 / Accepted: 1 December 2014 / Published online: 18 January 2015

Abstract Catalytic synthesis of some polysubstituted imidazoles under solvent-free condition is reported and their characterization has been carried out spectral techniques. Electronic spectral studies reveal that their solvatochromic behavior depends both the polarity of the medium and hydrogen bonding properties of the solvents. Specific hydrogen bonding interaction in polar solvents modulated the order of the two close lying lowest singlet states. The solvent effect on absorption and emission spectral results has been analyzed by multiple parametric regression analysis. Solvatochromic effects on the emission spectral position indicate the charge transfer (CT) character of the emitting singlet states both in a polar and a non polar environment. The fluorescence decays for the imidazoles fit satisfactorily to a bi exponential kinetics. These observations are in consistent with quantum chemical calculations.

Keywords Imidazoles · Indium trifluoride · Multiple parametric regression · CT

Introduction

Polysubstituted imidazole derivatives have been used as highly sensitive fluorescent chemosensor for sensing, imaging metal ions and play an vital role in material science due to their optoelectronic properties [1–4]. Its chelates with Ir^{3+} are major components for organic light emitting diodes [5]. Since they exert the properties of piezochromism, photochromism and thermochromism, they are used in molecular photonics [6]. Imidazole derivatives possess diverse biological activities, play important role as versatile building blocks for the synthesis of natural products [7–11]. Therefore, the synthesis of these imidazole derivatives has attracted much attention in organic synthesis.

The influence of solvents on emission spectra and quantum yields may have several origins like perturbation, due to the solvent refractive index and dielectric constant to hydrogen bonding and complexation between the fluorophore and the solvent [12]. These factors can change the energy difference between the ground (S_0) and the first excited (S_1) states and can shift the emission maxima or affect quantum yield. Solvent moderated shifts of the energy levels may enhance or inhibit radiationless transitions to the ground state via proximity effect [13].

Herein we report the synthesis of naphthyl substituted imidazole derivatives using indium trifluride (InF_3) as a highly efficient catalyst. The spectral characteristics of the synthesised imidazoles in solvents of different polarity and hydrogen bonding capacity have been discussed. The Lippert solvent parameter Δf, $E_T(30)$ polarity scale and the multiparameter Kamlet-Taft and Catalan solvent scales are used to describe the solvent effect on the fluorescence emission and Stokes shift of imidazole derivatives. We have also addressed the influence of solvents on the photophysical properties of the synthesized molecules in terms of $hc\tilde{\upsilon}_{abs}^{vac}$, $hc\tilde{\upsilon}_{flu}^{vac}$ and $(hc\tilde{\upsilon}_{abs}^{vac} - hc\tilde{\upsilon}_{flu}^{vac})$ with solvent polarity function.

Experimental

Spectral Measurements and Computational Details

The infrared spectra were recorded with an Avatar 330-Thermo Nicolet FT-IR spectrometer. The proton spectra at 400 MHz were obtained at room temperature using a Bruker

J. Jayabharathi (✉) · V. Thanikachalam · V. Kalaiarasi · P. Ramanathan
Department of Chemistry, Annamalai University, Annamalainagar 608 002, Tamilnadu, India
e-mail: jtchalam2005@yahoo.co.in

400 MHz NMR spectrometer. Proton decoupled ^{13}C NMR spectra were also recorded at room temperature employing a Bruker 400 MHz NMR spectrometer operating at 100 MHz. The mass spectra of the samples were obtained using a Thermo Fischer LC-Mass spectrometer in FAB mode. The UV-vis absorption and fluorescence spectra were recorded with PerkinElmer Lambda 35 spectrophotometer and PerkinElmer LS55 spectrofluorimeter, respectively. Fluorescence lifetime measurements were carried out with a nanosecond time correlated single photon counting (TCSPC) spectrometer Horiba Fluorocube-01-NL lifetime system with NanoLED (pulsed diode exCitation source) as the excitation source and TBX-PS as detector. The slit width was 8 nm and the laser excitation wavelength was 280 nm. The fluorescence decay was analyzed using DAS6 software. The quantum yield for all the imidazoles were measured in dichloromethane using coumarin 47 in ethanol as the standard [14–17]. The radiative and non-radiative rate constants, k_r and k_{nr}, were deduced from the quantum yield (Φ_f) and lifetime (τ) using the equation, $F_f = F_{isc}\{k_r/(k_r+k_{nr})\}$; Φ_{isc} is the intersystem crossing yield, $k_r = F_f/t, k_{nr} = 1/(\tau) - F_f/(\tau); (\tau) = (k_r+k_{nr})^{-1}$. The quantum chemical calculations were performed using the Gaussian-03 [18].

InF_3 Catalyzed Facile and Rapid Synthesis of Polysubstituted Imidazoles

A mixture of naphthaldehyde (1 mmol), benzil (1 mmol), substituted aniline (1 mmol), ammonium acetate (1 mmol) and InF_3 (1 mol%) was stirred at solvent-free conditions at 80 °C, progress of the reaction was monitored by TLC. After completion of the reaction, the mixture was cooled, dissolved in acetone and filtered. The product was purified by column chromatography using benzene: ethyl acetate (9:1) as the eluent.

*1-(Naphthalene-1-yl)-2,4,5-Triphenyl-1H-Imidazole (**1**)*

M.p. 251°., Anal. calcd. for $C_{31}H_{22}N_2$: C, 88.12; H, 5.25; N, 6.63; Found: C, 86.89; H, 4.02; N, 5.35. ^1H NMR (400 MHz, $CDCl_3$): δ, 7.92 (d, J=6.8Hz, 3H), 7.56 (d, J=6.4Hz, 6H), 7.43 (t, J=7.6Hz, 3H), 7.26–7.37 (m, 10H). ^{13}C NMR (100 MHz, $CDCl_3$ and DMSO):δ 125.68, 127.10, 128.11, 128.27, 128.33, 128.48, 130.01, 132.92, 146.13. MS: m/z. 422[M^+].

*2-(4-Fluorophenyl)-1-(Naphthalene-1-yl) -4,5-Diphenyl-1H-Imidazole (**2**)*

M.p. 244 °C, Anal. calcd. for $C_{31}H_{21}FN_2$: C, 84.52; H, 4.81; F, 4.31; N, 6.36; Found: C, 83.89; H, 3.82; F, 4.11; N, 5.15. ^1H NMR (400 MHz, $CDCl_3$): δ, 7.07 (t, J=8.4 Hz, 3H), 7.26–7.33 (m, 9H), 7.49 (d, J=6.8 Hz, 6H), 7.81 (t, J=7.6 Hz, 3H). ^{13}C NMR (100 MHz, $CDCl_3$ and DMSO): δ 115.87, 116.09, 12.14, 127.23, 127.32, 127.58, 127.84, 128.66, 145.20, 164.40, 167.61, 172.09, 184.56, 195.80. MS: m/z 440 [M^+].

*2-(4-Methoxyphenyl)-1-(Naphthalene-1-yl) -4,5-Diphenyl-1H-Imidazole (**3**)*

M.p. 254 °C, Anal. calcd. for $C_{32}H_{24}N_2O$: C, 84.93; H, 5.35; N, 6.19; O, 3.54, Found: C, 82.27; H, 4.27; N, 5.13; O, 3.21. ^1H NMR (400 MHz, $CDCl_3$): δ, 3.67 (s, 3H), 6.61 (d, J= 6.8 Hz, 2H), 7.56 (bs, 4H), 7.20–7.54 (m, 9H), 7.66–7.70 (m, 5H), 7.81 (bs, 2H). ^{13}C NMR (100 MHz, $CDCl_3$ and DMSO): δ 55.11, 113.49, 122.99, 123.20, 125.03, 126.57, 126.69, 127.27, 127.33, 127.46, 127.89, 128.08, 128.14, 128.20, 128.36, 128.83, 129.36, 129.49, 130.65, 130.71, 130.92, 131.07, 131.75, 132.47, 133.85, 133.94, 134.57, 138.03, 147.75, 159.54, 167.80. MS: m/z 452 [M^+].

*1-(Naphthalene-1-yl)-4,5-Diphenyl-2-(P-Tolyl)-1H-Imidazole (**4**)*

M.p. 241 °C, Anal. calcd. for $C_{32}H_{24}N_2$: C, 88.04; H, 5.54; N, 6.42; Found: C, 87.83; H, 5.32; N, 6.13. ^1H NMR (400 MHz, $CDCl_3$): δ, 2.18 (s, 3H), 7.79 (d, J=6.8 Hz, 2H), 7.67 (d, J= 6.8 Hz, 2H), 7.26–7.48 (m, 10H), 7.20 (d, J=7.2 Hz, 1H), 7.03 (d, J=8 Hz, 5H), 6.80 (d, J=7.6 Hz, 2H). ^{13}C NMR (100 MHz, $CDCl_3$ and DMSO): δ 21.21, 123.00, 125.04, 125.48, 126.63, 126.70, 127.28, 127.37, 127.48, 127.73, 127.94, 128.00, 128.12, 128.15, 128.24, 128.47, 128.81, 129.07, 129.38, 129.48, 130.67, 130.71, 131.10, 131.99, 133.84, 133.96, 134.60, 138.16, 138.19, 147.97. MS: m/z 436 [M^+].

*3-(1-(Naphthalen-1-yl)-4, 5-Diphenyl-1H- Imidazole-2-yl) Phenol (**5**)*

M.p. 263 °C, Anal. calcd. for $C_{31}H_{22}N_2O$: C, 84.91; H, 5.06; N, 6.39; O, 3.65, Found: C, 84.86; H, 4.98; N, 6.23; O, 3.21. ^1H NMR (400 MHz, $CDCl_3$): δ, 7.36–7.47 (m, 13H), 7.68 (d, J=6 Hz, 3H), 7.73 (d, J=5.6 Hz, 3H), 8.16 (d, J=4 Hz, 3H). ^{13}C NMR (100 MHz, $CDCl_3$ and DMSO): δ 126.50, 126.59, 127.42, 128.20, 128.29, 128.61, 128.68, 128.74, 128.82, 129.02, 130.41, 132.62, 136.82, 145.58, 160.19. MS: m/z 438 [M^+].

Result and Discussion

Solvent Modulated Absorption and Emission Behavior

Room temperature absorption and emission of naphthyl imidazole derivatives have been displayed in Fig. 1a. The absorption maxima is shifted from 281 to 324 nm in varying the

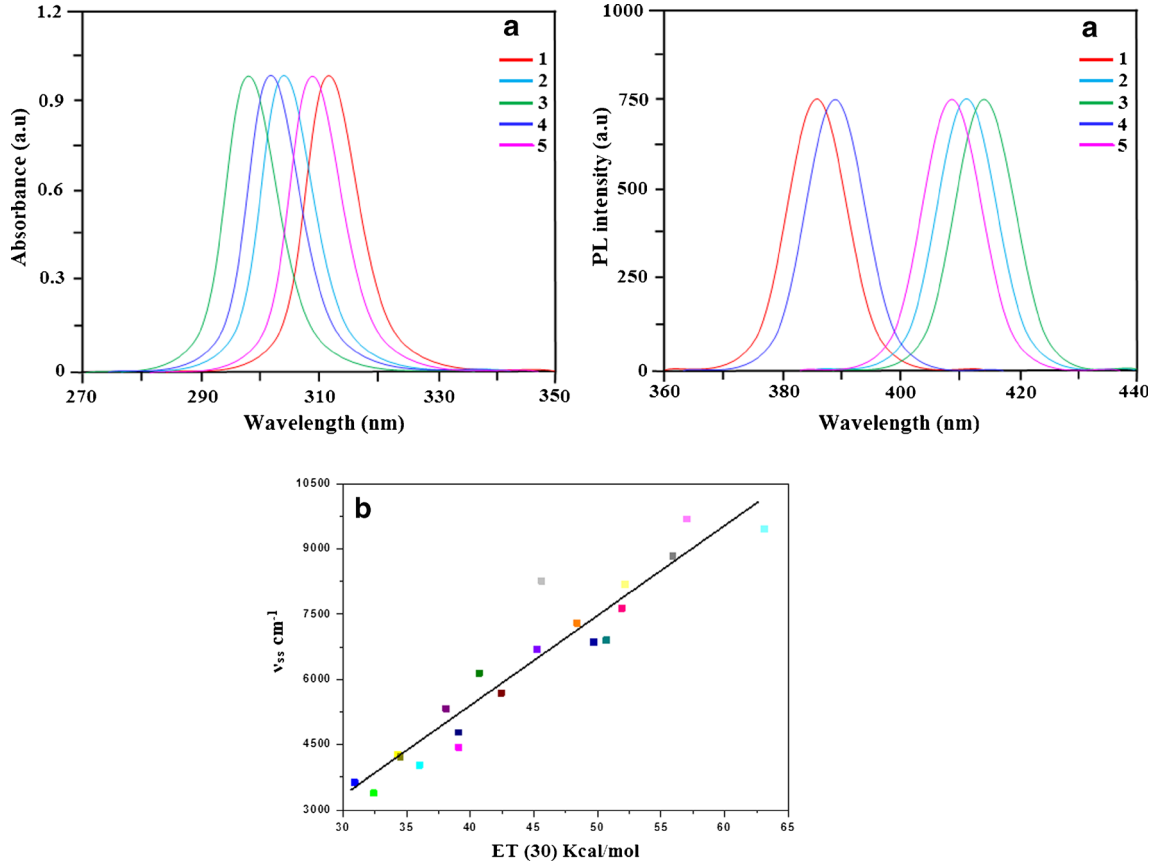

Fig. 1 **a** Absorption and emission spectra of naphthyl imidazole derivatives in dichloromethane; **b** Plot of Stokes shift (ν_{ss}) cm^{-1} Vs $E_T(30)$

polarity of the solvents which corresponds to π- π* transition. The magnitude of the shift suggests that the ground state of the molecule is polar. The emission spectra show a red-shifted band in the region of 323–435 nm on increasing the solvent polarity. The effect of polarity of the medium on the fluorescence maximum is more intense than that on the absorption maximum. This observation suggests that the emitting state is more polar than the ground state [19–21]. The linear variation of the Stokes shift with $E_T(30)$ has been shown in Fig. 1b. Increase of Stokes shift from non-polar to polar aprotic solvents mainly due to the combined effect of increasing the polarity of the medium and intramolecular charge transfer (CT) state. The influence on fluorescence emission in methanol-water mixture of different compositions has been monitored to understand the specific solvent-fluorophore interactions and the spectra are illustrated in Fig. 2a. The addition of water to methanol-water mixture enhances the fluorescence with red shift. This effect may be due to the combined

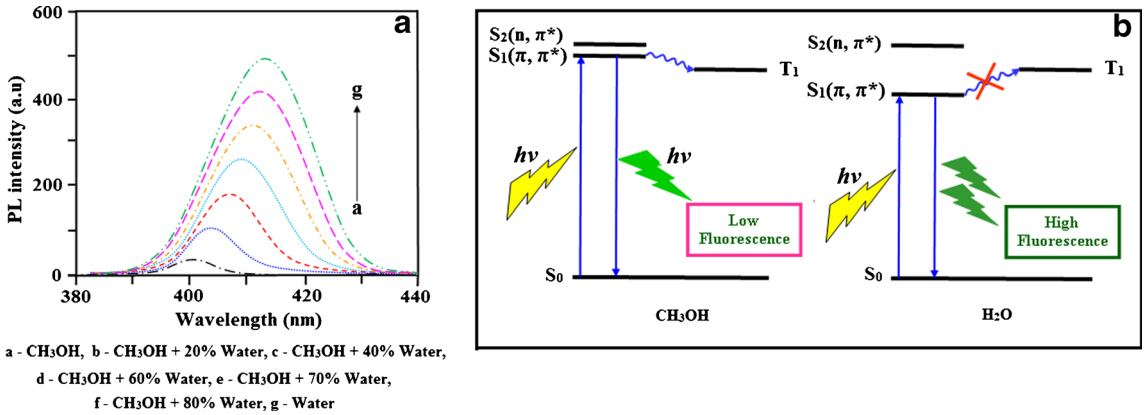

Fig. 2 **a** Emission profile of imidazole 1 in methanol as function of water composition; **b** Schematic demonstration of modulation of the close-lying lowest singlet n- π* and π - π* states with solvent polarity in the excited state

Table 1 Adjusted coefficients (($\upsilon_a)_0$, c_a, c_b and c_c) for the multilinear regression analysis of the absorption (υ_{ab}), fluorescence (υ_{fl}) wave numbers and Stokes Shift ($\Delta\upsilon_{ss}$) of imidazole derivatives (**1**–**5**) with solvent polarity/polarizability and acid and base capacity using the Taft (π*, α and β) and the Catalan (SPP^N, SA and SB) scales

	(υ_x)	($\upsilon_x)_0 cm^{-1}\times10^{-4}$	(π*)×10^{-4}	$c_\alpha\times10^{-4}$	$c_\beta\times10^{-4}$
1	υ_{ab}	3.13±0.03	−0.43±0.57	2.36±1.75	−2.00±1.33
	υ_{fl}	2.68±0.03	0.08±0.61	−1.45±1.88	1.29±1.42
	$\Delta\upsilon_{ss}$	0.45±0.06	−0.53±1.62	3.81±3.06	−3.29±2.73
2	υ_{ab}	3.25±0.02	−0.20±0.32	1.08±0.99	−0.84±0.75
	υ_{fl}	2.6±0.005	0.01±0.92	−1.22±2.81	1.09±2.31
	$\Delta\upsilon_{ss}$	0.64±0.06	−0.22±1.10	2.30±3.37	−1.94±2.56
3	υ_{ab}	3.25±0.04	−0.33±0.69	2.20±2.12	−1.19±1.61
	υ_{fl}	2.70±0.08	0.30±1.41	−3.26±4.33	3.00±3.28
	$\Delta\upsilon_{ss}$	0.56±0.11	−0.63±1.96	5.46±6.00	−4.89±4.55
4	υ_{ab}	3.25±0.04	−0.23±0.63	1.965±1.95	−1.80±1.48
	υ_{fl}	2.74±0.06	0.40±1.01	−3.01±3.11	2.54±2.36
	$\Delta\upsilon_{ss}$	0.51±0.09	0.63±1.62	4.98±4.95	−4.33±3.76
5	υ_{ab}	3.18±0.03	0.03±0.55	11.18±1.69	−1.16±1.28
	υ_{fl}	2.53±0.02	0.28±0.42	−1.65±1.30	1.38±0.99
	$\Delta\upsilon_{ss}$	0.65±0.05	−0.32±0.92	2.83±2.83	−2.44±2.14
	(υ_x)	**($\upsilon_x)_0 cm^{-1}\times10^{-4}$**	**$c_{SPP}^N\times10^{-4}$**	**$c_{SA}\times10^{-4}$**	**$c_{SB}\times10^{-4}$**
1	υ_{ab}	3.17±0.02	0.71±0.48	−1.55±1.29	0.96±0.84
	υ_{fl}	2.63±0.03	−0.96±0.08	1.86±1.39	−1.08±0.91
	$\Delta\upsilon_{ss}$	0.84±0.05	1.67±0.99	−3.41±2.66	2.08±1.74
2	υ_{ab}	3.27±0.01	−0.34±0.28	−0.56±0.75	0.29±0.49
	υ_{fl}	2.54±0.03	−0.12±0.07	2.71±2.02	−1.60±1.32
	$\Delta\upsilon_{ss}$	0.72±0.04	1.62±0.94	−3.27±2.50	1.89±1.63
3	υ_{ab}	3.30±0.003	9.30±5.75	−2.03±1.54	1.31±1.00
	υ_{fl}	2.58±0.063	−1.43±1.23	2.88±3.29	−1.68±2.15
	$\Delta\upsilon_{ss}$	0.72±0.08	2.36±1.71	−4.91±4.6	3.00±3.00
4	υ_{ab}	3.30±0.03	0.57±5.78	−1.08±1.55	0.63±1.01
	υ_{fl}	2.66±0.43	−1.67±0.85	3.22±2.27	−1.83±1.50
	$\Delta\upsilon_{ss}$	0.642±0.07	2.25±1.41	−4.30±3.77	2.46±2.46
5	υ_{ab}	3.22±0.023	0.77±0.45	−1.73±1.20	1.11±0.78
	υ_{fl}	2.50±0.002	-0.62±0.37	1.33±1.01	−0.80±0.66
	$\Delta\upsilon_{ss}$	0.07±0.04	1.40±0.78	−3.05±2.11	1.92±1.38

effect of hydrogen bonding and polarity of the medium. Mixing of two closely lying lowest singlet state (n, π*and π, π*) of imidazole derivatives favor the intersystem crossing [22]. As the polarity of the medium is increased, intermolecular hydrogen bonding interaction in the excited state stabilized the π- π* transition and the energy between the two states increased, which diminishes the mixing between the states (Fig. 2b). As a result intersystem crossing from S_1 to T_1 decreases and an enhancement of fluorescence is observed.

The spectral shift in fluorescence band may be due to the interaction between the dipole moment of the solute and polarizability of the solvent. The extent of charge separation on electronic excitation have been determined by change in the dipole moment ($\Delta\mu=\mu_e-\mu_g$) utilizing the spectral shift between the absorption and emission maxima as a function of solvent polarity. According to Lippert-Mataga equation [23], $\bar{v}_{ss} = \bar{v}_{ab} = \bar{v}_{fl} = const + \left[2\left(\mu_e-\mu_g\right)^2 / hca^3\right] f(\varepsilon,n)$, where $f(\varepsilon,n)=(\varepsilon-1)/(2\varepsilon+1)-(n^2-1)/(2n^2+1)$, the orientation polarizability of the solvent, n is refractive index, n is dielectric constant, μ_e and μ_g are dipole moments of the species in S_1 and S_0 states, respectively, h is Planck's constant, c is velocity of light and a is Onsager's cavity radius. The geometrical optimization was done by DFT method using Gaussian-03[18] to calculate the μ_g. Using the calculated μ_g value, [3.31 D (**1**), 3.64 D (**2**), 2.02 D (**3**), 3.33 D (**4**) and 4.09 D (**5**)] and the slope of Lippert-Mataga plot, the calculated μ_e is in the range, 12–16 D for the studied imidazoles.

Multiple linear regression analysis is performed to identify the different modes of solvation determining the absorption and emission energies. Kamlet and Taft [24] put forward $y = y_0+a_\alpha\ \alpha+b_\beta\ \beta+c_{\pi^*}\ \pi^*$(Kamlet-Taft), where π*, α and β parameters to characterize the polarity/polarizability, the acidity and the basicity of a solvent, respectively. Conversely, Catalan et al. [25] proposed an empirical solvent scales for polarity/polarizability (SPP), acidity (SA) and basicity (SB) to describe the respective properties of a given solvent, $y=y_0+a_{SA}SA+b_{SB}SB+c_{SPP}SPP$ (Catalan).

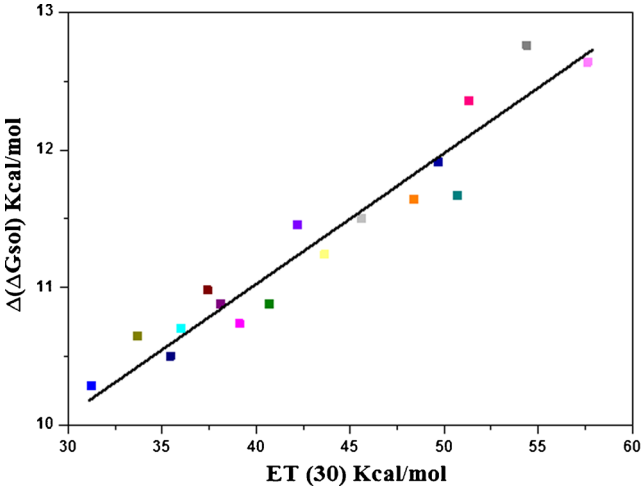

Fig. 3 Plot of Δ (ΔG_{solv}) of imidazole 1 Vs $E_T(30)$

The coefficients affecting the absorption and fluorescence of imidazole derivatives are displayed in Table 1. Kamlet negative coefficient of solvent dipolar interaction (π^*) and hydrogen bond accepting property (β) indicate these two parameters contribute to the stabilization of the ground state of imidazole derivatives. The coefficient controlling the H-donor capacity or acidity of the solvent [C_α] has a negative value. This indicates these parameters of the solvent stabilized the excited state. The coefficient representing the polarisability and electron releasing ability or basicity of the solvent has a negative value. The calculated ratio of β over π^* [$0.22(\upsilon_{abs})$ & $0.06(\upsilon_{emi})$ (**1**), $0.23(\upsilon_{abs})$ & $0.01(\upsilon_{emi})$ (**2**) 0.28 (υ_{abs}) & $0.10(\upsilon_{emi})$ (**3**), $0.13(\upsilon_{abs})$ & $0.15(\upsilon_{emi})$ (**4**), and $0.03(\upsilon_{abs})$ & $0.20(\upsilon_{emi})$ (**5**)] reveal that interactions between imidazole derivatives and solvents with hydrogen bond accepting property (β) predominates in the excited state. The free energy changes of solvation and reorganization energies in various solvents have been estimated by following the equation, $E(A)=\Delta G_{solv}+\lambda_1$ and $E(F)=\Delta G_{solv}-\lambda_0$, where E(A) and E(F) are absorption and fluorescence band maxima in cm^{-1}, respectively, ΔG_{solv} is the difference in free energy of the ground and excited states in a given solvent and λ represents the reorganization energy. Under the condition that $\lambda_0\lambda_1\lambda$, $E(A)+E(F)=2\Delta G_{solv}$; $E(A)-E(F)=2\lambda$. The ΔG_{solv} is maximum for hexane since it is purely non-polar and also α and β values of hexane are zero. The ΔG_{solv} is minimum in water. The differences between these values give the free energy change required for hydrogen bond formation. The plot of Δ (ΔG_{solv})=(ΔG_{hex}- ΔG_{water})

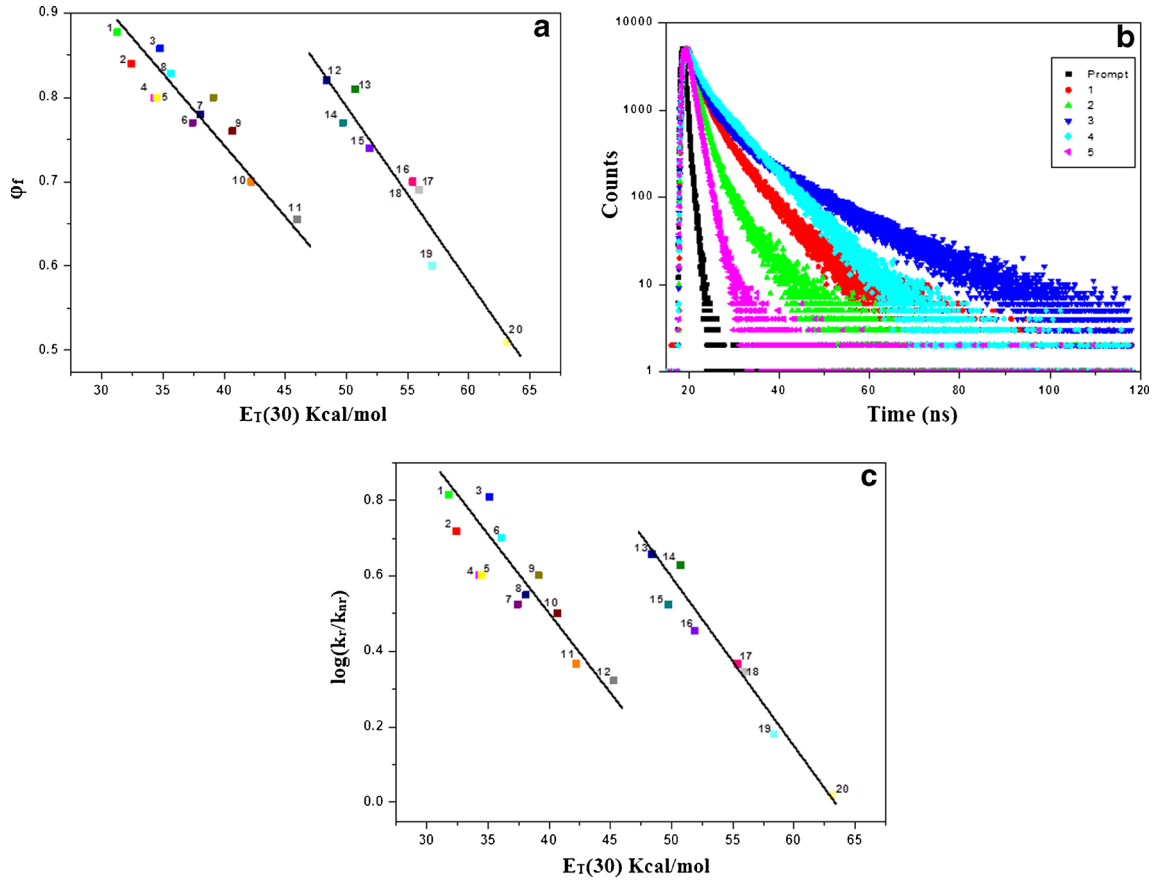

Fig. 4 **a** Plot of quantum yield of imidazole 1 with $E_T(30)$; **b** Lifetime curves of imidazoles1-5 in ethanol; **c** Plot of log (k_r/k_{nr}) Vs $E_T(30)$

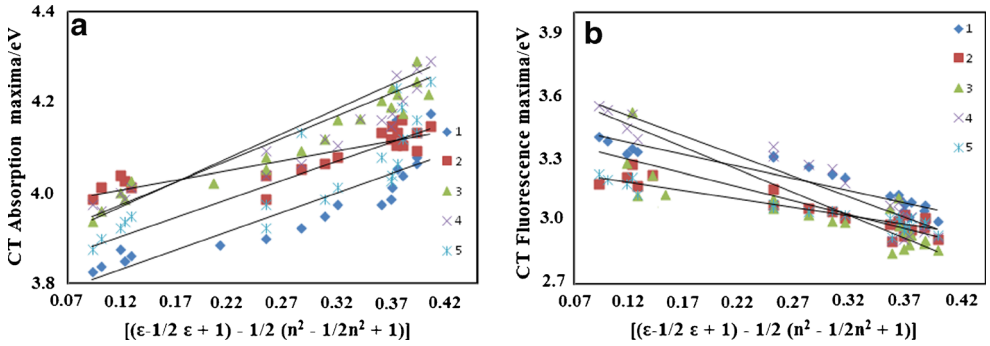

Fig. 5 **a** Plot of CT absorption maxima Vs solvent polarity function; **b** Plot of CT fluorescence maxima Vs solvent polarity function

versus $E_T(30)$ has been depicted in Fig. 3. The difference in free energy of solvation in hexane and different hydrogen bonding solvents follow the order of the hydrogen bond energy [26]. In aprotic solvents the values are small and interaction of imidazole derivatives with those solvents is purely due to dipolar interactions in the excited state. The definite values of reorganization energy confirmed the interaction between low frequency motions such as reorientation of solvent cell with low and medium frequency nuclear motion of the solute.

The variation of fluorescence quantum yield (φ_f) measured in solvents of different polarity with solvent polarity parameter E_T (30) is depicted in Fig. 4a. The increase of φ_f in polar protic medium is compared with that in polar aprotic medium. This may be due to differential contribution of CT and hydrogen bonding interactions. The calculated radiative and non-radiative rate constants from the quantum yield (Φ_f) and lifetime (τ) (Fig. 4b) are used to understand the effect of solvation on the dynamics of the excited state. The logarithm of (k_r/k_{nr}) is plotted against the solvent polarity parameter E_T (30) which is shown in Fig. 4c. Two different straight lines are obtained, one for aprotic solvents and the other for protic solvents. In both the cases, upon increasing the polarity the logarithm ratio of radiative to non-radiative rate decreases but a steeper slope is obtained for protic solvents. It indicates that the radiative and non-radiative rates are more sensitive toward protic solvents. It may be that the hydrogen bonding interaction in polar protic environment enhances the stabilization of the S_1 state as a result the non-radiative relaxation rate increases [27].

An interesting result is provided by the effect on the shift of the CT absorption bands with increasing solvent polarity (Fig. 5a) [28, 29]. With the assumption that point dipole is at the center of the spherical cavity and the mean solute polarizability (α) to be insignificant, it follows, $hc\widetilde{\upsilon}_{abs} \approx hc\widetilde{\upsilon}_{abs}^{vac} - 2\mu_g \left(\mu_e - \mu_g\right) / a_0^3[(\varepsilon - 1/2\varepsilon + 1) - {}^{1}/_{2}(n^2 - 1/2n^2 + 1)]$, where μ_g and μ_e are the dipole moments of the solute in the ground and excited states, correspondingly, ν_{abs} and are the spectral positions of a solvent-equilibrated absorption maxima and the value extrapolated to the gas-phase, respectively, a_o is the effective radius of the Onsager cavity [30] and ε and n are the static dielectric constant and the refractive index of the solvent, respectively. From the plot of energy with solvent polarity function, the values of μ_g (μ_e - μ_g) / and are determined and the μ_g values are displayed in Table 2. In the excited state, the negative and positive ends of the electric dipole are localized nearly in the centers of the donor and acceptor fragments respectively. A considerable shift of their spectral position, increase of Stokes shift and enlargement of emission bandwidth with increasing solvent polarity in fluorescence spectra point to the CT character of fluorescent states. The excited state dipole moments μ_e can be estimated by the fluorescence

Table 2 Slopes and intercepts of the solvatochromic plots of the CT fluorescence, lifetime (τ) and dipole moments (D) of imidazoles

Compd.	Nonpolar solvents and Polar solvents		Polar solvents		τ, ns	Dipole moment μ_g/μ_e
	hc_{abs}^{vac}, eV	μ_e (μ_e - μ_g) / a_0^3 eV	hc_{abs}^{vac}, eV	μ_e (μ_e - μ_g) / a_0^3 eV		
1	2.91	1.38	2.99	1.41	**2.77**	3.0/5.6
2	3.42	1.87	3.49	1.90	2.14	3.3/6.0
3	3.32	1.71	3.41	1.83	3.99	4.1/6.8
4	3.50	1.60	3.52	1.68	4.01	3.6/6.2
5	3.58	1.42	3.60	1.50	1.42	2.0/5.1

solvatochromic shift method due to the fact that the excited states live sufficiently long with respect to the orientation relaxation time of the solvent [31–34]. Under the same assumption as used for absorption, it follows that, $hc\widetilde{\upsilon}_{flu} \approx hc\widetilde{\upsilon}_{flu}^{vac} - 2\mu_e\left(\mu_e - \mu_g\right) / a_0^3[(\varepsilon - 1/2\varepsilon + 1) - {}^1/_2 (n^2 - 1/2n^2 + 1)]$, where υ_{flu} and are the spectral positions of the solvent equilibrated fluorescence maxima and the value extrapolated to the gas-phase, respectively. The compounds studied show a satisfying linear correlation between the energy $hc\upsilon_{flu}$ and the solvent polarity function in a polar environment and also in all the solvents (Fig. 5b) [35]. The value of μ_e (μ_e - μ_g)/ are displayed in Table 2. The values extracted from the data measured in polar media are somewhat larger than those resulting from the analysis of the data obtained for the whole range of the solvents. This can be explained only by the dependence of the electronic structure of the fluorescent states on solvation. Due to a relatively small energy gap between the lowest internal charge transfer (ICT) states and the states excited locally in the nonpolar solvents, lead to increase the contribution of (π π*) character to the wave function of the CT states. It leads to lowering of energy with respect to a pure CT state because of a stabilizing character of such interactions and red shift obtained in the fluorescence spectra. Under the assumption that the CT fluorescence corresponds to the state reached directly upon excitation, the quantity (μ_e - μ_g) ^{2}/ can be evaluated from the solvation effect on the Stokes shift, $hc\left(\widetilde{\upsilon}_{abs} - \widetilde{\upsilon}_{flu}\right) = hc\left(hc\widetilde{\upsilon}_{abs}^{vac} - hc\widetilde{\upsilon}_{flu}^{vac}\right) + 2\left(\mu_e - \mu_g\right)^2 / [(\varepsilon - 1/2\varepsilon + 1) - (n^2 - 1/2n^2 + 1)]$. The compounds studied show a satisfying linear correlation between the energy hc $\widetilde{\upsilon}$ $_{abs}$ - hc $\widetilde{\upsilon}$ $_{flu}$ and the solvent polarity function in a polar environment and also in all the solvents studied; the values of $(\mu_e - \mu_g)/a_0^3$ are 1.38 eV (**1**), 1.87 eV (**2**), 1.71 eV (**3**), 1.60 eV (**4**) and 1.42 eV (**5**). Under the assumption that $\mu_e >> \mu_g$ and with the effective spherical radius (a_0) of the molecules as estimated from the molecular dimensions of the compounds calculated by molecular mechanics are 6.03 A° (**1**), 6.09 A° (**2**), 6.18 A° (**3**), 6.11 A° (**4**) and 6.10 A° (**5**) values of μ_e are of 5.6 D (**1**), 6.0 D (**2**), 6.8 D (**3**), 6.2 D (**4**) and 5.1 D (**5**).

Conclusion

Kamlet-Taft analysis shows that imidazole derivatives in the excited state form a stable complex with solvents with high hydrogen bond acceptance abilities. These compounds show a satisfying linear correlation between the energies viz., hc $\widetilde{\upsilon}$ $_{abs}$, hc $\widetilde{\upsilon}$ $_{flu}$, hc $\widetilde{\upsilon}$ $_{abs}$ - hc $\widetilde{\upsilon}$ $_{flu}$ and the solvent polarity function. Hydrogen bonding interaction in protic polar environment enhances the stabilization of S_1 state which leads to reduce the mixing between the states and as a result decrease of non-radiative relaxation is observed. The theoretical results based on density functional theory are in good agreement with experimental results.

Acknowledgments One of the authors Prof. J. Jayabharathi is thankful to DST [No. SR/S1/IC-73/2010], DRDO (NRB-213/MAT/10–11), UGC (F. No. 36–21/2008 (SR)) and CSIR (NO 3732/NS-EMRII) for providing funds to this research study.

References

1. Lefebvre JF, Leclercq D, Gisselbrecht JP, Richeter S (2010) Synthesis, characterization, and electronic properties of metalloporphyrins annulated to exocyclic imidazole and imidazolium rings. Eur J Org Chem 1912–1920
2. Shi L, Su J, Wu Z (2011) Inorg Chem 50:5477–5484
3. Adachi M, Nagao M (2001) Design of near-infrared dyes based on pi-conjugation system extension 2. Theoretical elucidation of framework extended derivatives of perylene chromophore. Chem Mater 13:662–669
4. Hung WS, Lin JT, Chien CH, Tao YT, Sun SS, Wen YS (2004) Highly phosphorescent bis-cyclometalated iridium complexes containing benzoimidazole-based ligands. Chem Mater 16:2480–2488
5. Chen CH, Shi J (1998) Review as emitting material for electroluminescence. Coord Chem Rev 171:161–174
6. Fridman N, Kaftory M, Speiser S (2007) Structures and photophysics of lophine and double lophine derivatives. Sensors Actuators B 126: 107–115
7. Golan DE, Armstrong AW (2007) Principles of pharmacology: The pathophysiologic basis of drug therapy. Wolters Kluwer Health
8. Bhat NR, Zhang PS, Mohanty SB (2007) p38 MAP kinase regulation of oligodendrocyte differentiation with CREB as a potential target. Neurochem Res 32:293–302
9. Lombardino JG, Wiseman EH (1974) Preparation and anti inflammatory activity of some non acidic trisubstituted imidazoles. J Med Chem 17:1182–1188
10. Misono M (2011) Unique acid catalysis of heteropoly compounds (heteropolyoxometalates) in the solid state. Chem Commun 1141–1152
11. Chang LL, Sidler KL, Cascieri MA, de Laszlo S, Koch G, Li B, MacCoss M, Mantlo N, Okeefe S, Pang M, Rolando A, Hagmann WK (2001) Bioorg Med Chem Lett 11:2549–2553
12. Lakowicz JR (2006) Principles of fluorescence spectroscopy, 3rd edn. Springer, New York
13. Lim EC (1986) J Phys Chem 90:6770–6777
14. Okada S, Okinaka K, Iwawaki H, Furugori M, Hashimoto M, Mukaide T, Kamatani J, Igawa S, Tsuboyama A, Takiguchi T, Ueno K (2005) Substituent effects of iridium complexes for highly efficient red OLEDs. Dalton Trans 9:1583–1590
15. Jayabharathi J, Thanikachalam V, Jayamoorthy K, Srinivasan N (2013) Synthesis, spectral studies and solvatochromism of some novel imidazole derivatives—ESIPT process. Spectrochim Acta Part A 105:223–228
16. Jayabharathi J, Thanikachalam V, Sathishkumar R, Jayamoorthy K (2012) Fluorescence investigation of the interaction of 2-(4-fluorophenyl)-1-phenyl-1H-phenanthro [9,10-d] imidazole with bovine serum albumin. Photochem Photobiol B 117:222–227

17. Jayabharathi J, Thanikachalam V, Sathishkumar R, Jayamoorthy K (2013) Physico-chemical studies of fused phenanthrimidazole derivative as sensitive NLO material. Spectrochim Acta Part A 101:249–253
18. Frisch MJ, Trucks GW, Schlegel HB, Scuseria GE, Robb MA, Cheeseman JR, Montgomery JA Jr, Vreven T, Kudin KN, Burant JC, Millam JM, Iyengar SS, Tomasi J, Barone V, Mennucci B, Cossi M, Scalmani G, Rega N, Petersson GA, Nakatsuji H, Hada M, Ehara M, Toyota K, Fukuda R, Hasegawa J, Ishida M, Nakajima T, Honda Y, Kitao O, Nakai H, Klene M, Li X, Knox JE, Hratchian HP, Cross JB, Bakken V, Adamo C, Jaramillo J, Gomperts R, Stratmann RE, Yazyev O, Austin AJ, Cammi R, Pomelli C, Ochterski JW, Ayala PY, Morokuma K, Voth GA, Salvador P, Dannenberg JJ, Zakrzewski VG, Dapprich S, Daniels AD, Strain MC, Farkas O, Malick DK, Rabuck AD, Raghavachari K, Foresman JB, Ortiz JV, Cui Q, Baboul AG, Clifford S, Cioslowski J, Stefanov BB, Liu G, Liashenko A, Piskorz P, Komaromi I, Martin RL, Fox DJ, Keith T, Al-Laham MA, Peng CY, Nanayakkara A, Challacombe M, Gill PMW, Johnson B, Chen W, Wong MW, Gonzalez C, Pople JA (2004) Gaussian 03 (Revision E.01). Gaussian, Inc, Wallingford
19. Pramanik S, Banerjee P, Sarkar A, Mukherjee A, Mahalanabis KK, Bhattacharya SC (2008) Spectroscopic investigation of 3-pyrazolyl 2-pyrazoline derivative in homogeneous solvents. Spectrochim Acta Part A 71:1327–1332
20. Willard DM, Riter RE, Levinger NE (1998) Dynamics of polar solvation in lecithin/water/cyclohexane reverse micelles. J Am Chem Soc 120:4151–4160
21. Saha S, Samanta A (2002) Influence of the structure of the amino group and polarity of the medium on the photophysical behavior of 4-amino-1,8-naphthalimide derivatives. J Phys Chem A 106:4763–4771
22. de Melo JSS, Becker RS, Macanita AL (1994) J Phys Chem 98: 6054–6058
23. Lippert E (1957) Spektroskopische bistimmung des dipolmomentes aromatischer verbindugen im ersten angeregten singulettzustand. Z Electrochem 61:962–975
24. Kamlet MJ, Taft RW (1976) The solvatochromic comparison method. 1. The scale of solvent hydrogen-bond acceptor (HBA) basicities. J Am Chem Soc 98:377–383
25. Catalan J, Lopez V, Perez P (1996) Use of the SPP scale for the analysis molecular system with dual emissions resulting from the solvent polarity. J Fluoresc 6:15–22
26. Castellan GW (1985) Physical chemistry, 3rd edn. Narosa Publishing House, Delhi
27. Dhar S, Rana DK, Roy SS, Roy S, Bhattacharya S, Bhattacharya SC (2012) Effect of solvent environment on the photophysics of a newly synthesized bioactive 7-oxy(5-selenocyanato-pentyl)-2H-1-benzopyran- 2-one. J Lumin 132:957–964
28. Rettig W, Zander M (1982) On twisted intramolecular charge transfer (TICT) stated in N-aryl-carbazoles. Chem Phys Lett 87:229–234
29. Chiba K, Aihara JI, Araya K, Matsunaga Y (1980) Bull Chem Soc Jpn 53:1703
30. Onsager L (1936) Electric moments of molecules in liquids. J Am Chem Soc 58:1486–1493
31. Böttcher CJF (1973) In: Van Belle OC, Bordewijk P, Rip A (eds) Theory of electric polarization, vol I. Elsevier, Amsterdam
32. Lippert EZ (1955) Naturforsch A10:541–545
33. Mataga N, Kaifu Y, Koizumi M (1955) The solvent effect on fluorescence spectrum. change of solute-solvent interaction during the lifetime of excited solute molecule. Bull Chem Soc Jpn 28:690–691
34. Liptay W (1974) In: Lim EC (ed) Excited states. Academic, New York, p 129
35. McRae EG (1957) Theory of solvent effects on molecular electronic spectra. Frequency shifts. J Phys Chem 61:562–572